https://doi.org/10.5194/egusphere-2026-3749
Preprint. Discussion started: 14 July 2026

Quantifying and Predicting Austral Summer Mesopause Height with a Temperature-Based Upwelling Proxy

Liang Zhang[1], Zhongfang Liu[1], Yajun Zhu[2]

[1]State Key Laboratory of Marine Geology, Tongji University, Shanghai, 200092, China
[2]State Key Laboratory of Solar Activity and Space Weather, National Space Science Center, Chinese Academy of Sciences, Beijing, 100190, China

Correspondence to: Liang Zhang (Liangzhang420@tongji.edu.cn)

Abstract. The mesopause, the coldest region of Earth's atmosphere near 85-100 km, is the boundary between mesosphere and thermosphere, yet its variability remains poorly quantified. Using 24 years (2002-2025) of the Sounding of the Atmosphere using Broadband Emission Radiometry (SABER) temperature measurements, we show that the high-latitude austral summer mesopause height is closely linked to the T80 index—a temperature- based proxy at 80 km for the strength of summer polar upwelling. On interannual timescales, the T80 index is almost perfectly correlated with the December mesopause height across 30°S–80°S, with a correlation coefficient (R) of 0.98 and a sensitivity of 0.36 km K^{-1} at 60°S. On daily timescales, this relationship weakens but remains significant (R = 0.48) at latitudes poleward of 55°S. The temperature field exhibits a vertical dipole response to T80 index: stronger upwelling (lower T80) induces adiabatic cooling below ~90 km and chemical/radiative heating above ~90 km through bottom-up coupling among dynamical, microphysical, and chemical processes. This dipole temperature response shifts the temperature profile downward, thereby lowering the mesopause height. The strong month-to-month persistence of both the T80 index and mesopause temperature provides substantial predictive skill, enabling one-month-ahead forecast of December mesopause height with correlation up to 0.90. Our results indicate that internal dynamics dominate the interannual summer mesopause variability, while signals of 11-year solar cycle and long-term CO_2 cooling cannot be reliably isolated from the 24-year observations.

1 Introduction

The mesopause, defined as the altitude of minimum temperature near 85-100 km altitude, is the transition between the mesosphere and the thermosphere (*Plane et al.*, 2023). The summer polar mesopause is the coldest region in Earth's atmosphere, with temperatures as low as 130 K (*Sheese et al.*, 2011; *Yi et al.*, 2021), owing to the adiabatic cooling of gravity wave-driven upwelling (*Garcia and Solomon*, 1985; *Holton*, 1983; *Lindzen*, 1981). The temperature and height of the mesopause are fundamental parameters that define the structure and dynamics of the near-space environment. The mesopause height exhibits a pronounced hemispheric and seasonal asymmetry: during solstices, it is significantly lower and

https://doi.org/10.5194/egusphere-2026-3749
Preprint. Discussion started: 14 July 2026

colder in the summer high-latitude hemisphere (~85-90 km) and higher and warmer elsewhere (~97-100 km) (*She and von Zahn*, 1998; *Xu et al.*, 2007).

The mesopause height serves as a critical reference level for multiple phenomena, and investigating its variability and controlling factors is essential for studies of the upper mesosphere and lower thermosphere. For instance, the peak altitude of polar mesospheric clouds (PMCs) is consistently observed ~3-4 km below the mesopause, indicating a tight coupling between the thermal structure and cloud microphysics (*Li et al.*, 2024; *Russell III et al.*, 2010). The peak altitude and density of the sodium layer are also influenced by mesopause height and temperatures (*Plane et al.*, 1999; *Zhou et al.*, 2005). *Siskind et al.* (2012) showed that the interannual variability in summer mesopause temperatures affects the zonal mean circulation in the lower thermosphere up to at least 115 km.

The primary driver and predictability of the summer mesopause height remain ambiguous. Traditionally, gravity wave breaking and dissipation are considered the dominant processes shaping the mesopause, yet significant underestimation exists between satellite observations and simulated mesopause heights in the summer polar region (*Pramitha et al.*, 2025). *Wang et al.* (2022) used CO_2 as a dynamical tracer and found that the mesopause height closely follows the signature of the residual circulation, particularly the region of strong upwelling, implying a circulation-dominated control. However, the specific mechanisms translating dynamic forcing into large-scale interannual changes in mesopause height have not been well quantified.

Using Na lidar measurements at midlatitudes, *She et al.* (2019) reported a cooling trend of ~1.85 K decade^{-1} near the mesopause and a solar response of ~5 K per 100 solar flux unit (sfu), and *Yuan et al.* (2019) reported that the non-summer mesopause descended at a rate of −450 m decade^{-1} and the summer mesopause by −130 m decade^{-1}. Using SABER satellite observations, *Zhao et al.* (2020) revealed a mesopause temperature cooling trend of −0.75 K decade^{-1} and a positive solar response of ~4 K (100 sfu)$^{-1}$ across all latitudes, and *Tang et al.* (2016) found that the mesopause temperature is sensitive to solar 11-year cycle but the mesopause height is insensitive. Many studies have examined how the mesopause responds to external forcings such as solar 11-year cycle and CO_2 cooling. However, investigations on internal mesospheric dynamical forcing remain limited.

This study investigates the interannual variations of mesopause driven by summer polar upwelling. The T80 index, defined as the temperature near 80 km over the summer polar region, serves as a proxy for the strength of the summer polar upwelling (*Zhang and Liu*, 2026; *Zhang et al.*, 2025b; *Zhang et al.*, 2025c). *Zhang et al.* (2025c) demonstrated that the mesospheric climate exhibits an interhemispheric anti-phase pattern during solstice months. In particular, the upwelling drives a vertical dipole response of temperatures at the summer polar region, through a bottom-up mechanism. Explicitly, a stronger upwelling causes lower temperature below ~90 km via adiabatic cooling, and higher temperature above ~90 km via coupled dynamical, microphysical, chemical, and thermal processes involving water vapor (H_2O), hydrogen (H), ozone (O_3), and oxygen (O). This dipole response of temperatures—cooling below and warming above 90 km—alters the vertical temperature profile and thus shifts the altitude of the cold-point mesopause. Within this framework, PMCs play an important

https://doi.org/10.5194/egusphere-2026-3749
Preprint. Discussion started: 14 July 2026

role in modulating H_2O distribution via a cold-trap effect, causing a hydration below PMCs and dehydration above PMCs (*Zhang et al.*, 2025a; *Zhang et al.*, 2025c). The cold-trap effect results from the charged meteoric smoke particle scheme for PMC formation, which assumes that charged meteoric smoke particles act as ice nuclei and ice particles grow in situ (*Zhang et al.*, 2025a; *Zhang et al.*, 2022). The dehydration above PMCs could influence the O_3 abundance (*Siskind et al.*, 2018), and the chemical/radiative heating of O_x (O_3 and O) is essential for the energy budget of mesopause (*Wu et al.*, 2026).

This study addresses three specific questions: (1) What quantitatively controls the interannual variability of the summertime high-latitude mesopause height in the SH? (2) What is the underlying physical mechanism linking this control to the observed height changes? (3) Based on this mechanism, can the summertime mesopause height be predicted on sub-seasonal to seasonal timescales?

Using nearly two decades of satellite observations, we test the hypothesis that the T80 index is the primary predictor of the austral summer mesopause height. We systematically quantify their relationship, elucidate the associated dynamical mechanism, and explore the potential for a statistical forecast. By answering these questions, this work aims to quantify the dominant role of internal forcing (summer polar upwelling) on mesopause height, and to assess whether external forcings (11-year solar cycle and long-term CO_2 cooling) can be detected within the current observational record.

2 Data and method

2.1 Multi-satellite Observations

This study utilizes temperature measurements from two complementary satellite instruments, the SABER and the Microwave Limb Sounder (MLS), to ensure long-term, consistent data coverage for interannual analysis.

The SABER instrument is onboard the NASA TIMED satellite, launched on 7 December 2001 into a 74.1° inclination orbit. The instrument operate on a 60-day yaw cycle that alternates its hemispheric coverage between 83°N-53°S and 53°N-83°S (*Russell et al.*, 1999). During the austral summer (e.g., November-December), the Southern Hemisphere (SH) high latitudes poleward of 53°S are optimally observed. We employ SABER version 2.07 level-2 temperature data spanning 2002-2025 (*Remsberg et al.*, 2008). As validated by *Liu et al.* (2026), SABER temperatures exhibit excellent long-term stability across the mesopause layer. Benefiting from a fine vertical resolution of ~2 km, SABER data are primarily used here to resolve the altitude of the cold-point mesopause.

Launched in 2004, the Aura/MLS instrument offers nearly-global coverage from 82°N to 82°S. We use MLS version 5 temperature data, with a typical single-profile precision of 3 K (*Jiang et al.*, 2007; *Schwartz et al.*, 2008). MLS offers robust, uninterrupted sampling over the austral summer high latitudes and therefore serves as the core dataset for calculating and analyzing the interannual variability of the T80 index.

https://doi.org/10.5194/egusphere-2026-3749
Preprint. Discussion started: 14 July 2026

2.2 The T80 Upwelling index

Direct long-term measurements of summer polar upwelling are unavailable, as mesospheric vertical winds are typically only a few cm s^{-1} (*Smith*, 2012). We therefore employ the T80 index, defined as the zonal-mean temperature near 80 km over the summer polar region (*Zhang et al.*, 2025c). This index serves as a robust proxy for the intensity of gravity wave-driven residual circulation upwelling: a lower T80 value indicates stronger adiabatic cooling and thus stronger upwelling. *Zhang and Liu* (2026) justified the choice of the 80 km level mainly based on two considerations: (1) the extremely low ozone concentration at this altitude renders radiative and chemical heating negligible, ensuring that temperature is dominated by adiabatic processes; (2) the high cross-instrument consistency for temperature measurements at this altitude (*García-Comas et al.*, 2014) enables reliable multi-satellite comparison. The T80 index for November, December, and January is derived from SABER and MLS data, as listed in Table 1.

A critical step for constructing a continuous, long-term T80 time series is to reconcile data from SABER and MLS, which have different observation patterns. SABER's yaw cycle introduces significant year-to-year variations in high-latitude coverage. As shown in Figure 1, full monthly December observations over 53°S-83°S are available before 2019, after which coverage gradually declines. Observation days in November increase from the 10 days in 2002 to 30 days in 2019, while those in January decrease from the 15 days in 2003 to 0 days in 2016.

We calculate the monthly mean T80 index separately from SABER and MLS data for November, December, and January. The right panels of Fig. 1 (d-f) show the consistency between the independently derived SABER (blue) and MLS (red) T80 time series. Although the SABER T80 is warmer than the MLS T80 by ~4.7 K in December, their interannual variability is highly consistent. Correlation coefficients between the two datasets for each month yield values of 0.93 (November), 0.99 (December), and 0.91 (January).

This significant linear relationship validates the T80 index as a highly consistent observable across different sensing technologies. Crucially, it allows us to calibrate and extend the T80 record. Using the derived linear regression equations, we can reliably estimate MLS-equivalent T80 values for periods with SABER data but no MLS data (specifically 2002-2003, prior to Aura's launch). The fitted values for December 2002 and 2003 are 177.5 K and 177.9 K, and for January 2003 and 2004 are 177.2 K and 176.4 K, respectively.

For all subsequent analyses of interannual variations, we therefore utilize a fused T80 index time series. This series is based primarily on the direct MLS T80 index (2004-2025), extended back to 2002-2003 using the calibrated values from SABER values. This approach mitigates the sampling limitations of either instrument alone and provides a consistent, 24-year (2002-2025) dataset for robust climate analysis.

https://doi.org/10.5194/egusphere-2026-3749
Preprint. Discussion started: 14 July 2026

Table 1. The monthly mean T80 index (unit: K) in November, December, and January obtained from SABER and MLS data from 2002 to 2025. The T80 index is the monthly and zonal mean temperature data at 0.0215 hPa from 75°S to 83°S.

	November (K)		**December (K)**		**January (K)**	
Year	SABER	MLS	SABER	MLS	SABER	MLS
2002	184.3		182.4			
2003	191.9		182.9		182.0	
2004	185.6	189.0	180.9	176.4	181.3	
2005	184.4	184.2	182.4	177.7	177.6	173.8
2006	195.3	191.6	184.1	180.0	180.6	176.2
2007	198.3	193.8	189.5	185.4	181.9	175.8
2008	199.0	193.4	189.6	184.9	183.2	177.1
2009	185.5	187.5	182.6	177.9	182.1	176.0
2010	201.9	197.3	192.3	187.4	176.3	172.3
2011	189.7	189.7	188.1	183.5	182.7	176.8
2012	185.9	183.8	177.6	172.6	183.0	177.4
2013	185.7	183.0	178.0	174.1	176.6	173.7
2014	189.7	186.6	185.5	181.4	178.9	175.1
2015	196.9	193.7	190.1	185.6	180.1	176.9
2016	185.0	182.0	177.7	172.6	182.8	177.5
2017	189.2	185.2	184.0	179.1		174.5
2018	192.6	188.4	183.7	178.4		175.2
2019	184.5	179.9	180.0	175.1		176.5
2020	200.6	196.8	193.6	187.8		176.2
2021	200.7	197.5	193.5	187.4		177.6
2022	197.9	194.4	190.5	184.3		179.2
2023	196.6	192.7	194.8	186.7		179.9
2024	194.1	190.5	192.6	184.6		178.9
2025	189.1		183.4			175.0

https://doi.org/10.5194/egusphere-2026-3749
Preprint. Discussion started: 14 July 2026

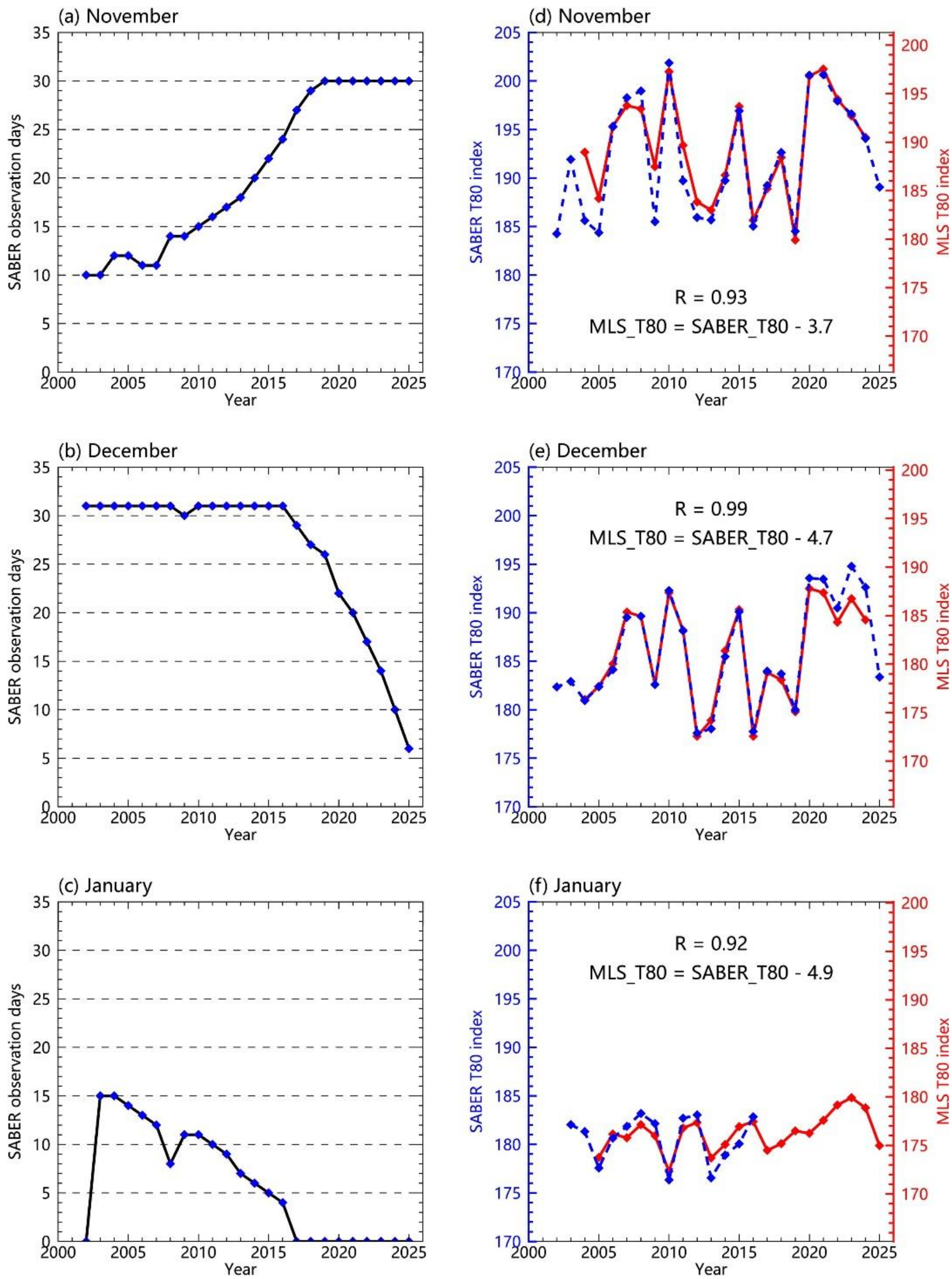

Figure 1. Comparison between the T80 index obtained from MLS and SABER data. The left panels show the available days of SABER observations at 53°S-83°S in (a) November, (b) December, and (c) January. The right panels show the relationships of the T80 calculated by MLS (red dashed lines) and SABER (blue solid lines) in (d) November, (e) December, and (f) January. The T80 index is calculated at 0.0215 hPa between 75°S and 83°S for SABER and MLS.

https://doi.org/10.5194/egusphere-2026-3749
Preprint. Discussion started: 14 July 2026

3 Results

3.1 Climatological structure and latitudinal variability of the mesopause

Before examining the interannual relationship between the T80 index and the mesopause, we first establish the climatological background of the mesopause during the austral summer using the SABER data. Figure 2 presents the zonal-mean temperature distribution in December, with the cold-point mesopause height marked by the dashed curve and its interannual standard deviation indicated by vertical error bars.

In the SH high latitudes (poleward of 35°S), the mesopause is located at relatively low altitudes, decreasing from ~91 km at 80°S to a minimum of ~88 km near 50°S. Equatorward of this minimum, the mesopause rises sharply, reaching 97–100 km between 30°S and 50°N. This distinct double- mesopause structure—a lower mesopause at summer high latitudes and a higher mesopause at lower latitudes—is consistent with previous climatological studies (*She and von Zahn*, 1998; *Xu et al.*, 2007).

The error bars in Fig. 2 further reveal a remarkable latitudinal structure in the interannual variations of the mesopause height. The standard deviation is modest (~1.2 km) at 80°S, increases gradually to a maximum of ~2.5 km near 40°S–50°S, and then drops to less than 1 km between 25°S and 50°N. This pattern indicates that the mesopause height varies most strongly not at the pole, but rather in the transition zone between the two mesopause regimes. In the following section, we quantify the variability of mesopause height using the T80 index as a proxy for the intensity of summer polar upwelling.

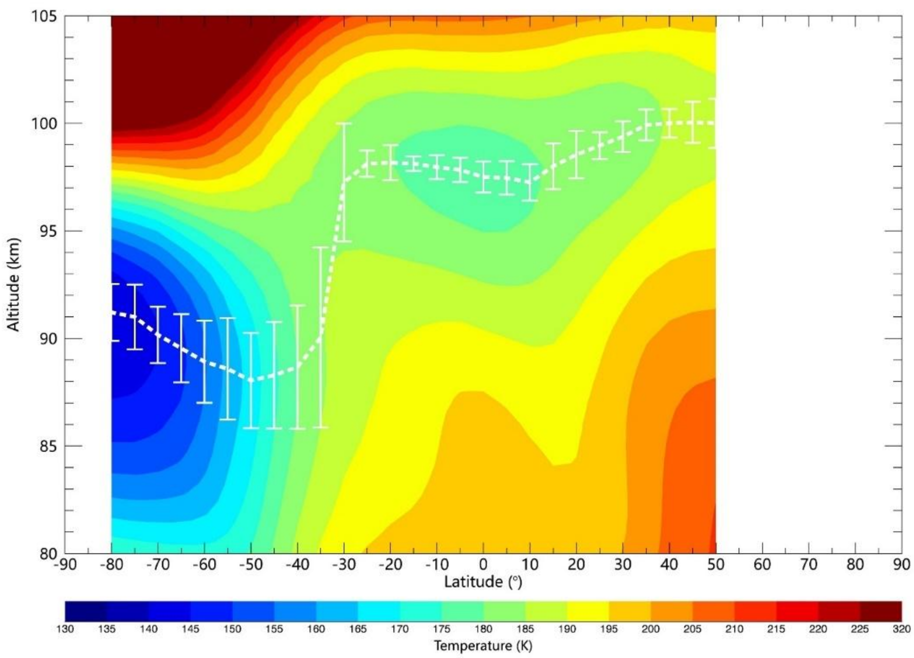

Figure 2. Climatological temperature distribution and mesopause height in December using SABER data (2002-2025). The dashed curve denotes the climatological mesopause height, and error bars indicate interannual standard deviation.

https://doi.org/10.5194/egusphere-2026-3749
Preprint. Discussion started: 14 July 2026

3.2 The T80-mesopause linkage on interannual scales

Figure 3 quantifies the interannual control of the SH summer mesopause height by the T80 index, showing their in-phase co-variability at 60°S in December from 2002 to 2024. Note that for 2021–2024, the SABER-derived mesopause height is based on fewer than 20 days of observational coverage per December due to satellite orbital shifts. The near-perfect visual agreement is confirmed by an extremely high linear correlation coefficient of R = 0.98. A least-squares linear fit yields: Mesopause Height (km) = 23.40 + 0.36 × T80, indicating a local sensitivity of approximately 0.36 km per Kelvin change in the T80 index. The interannual variability (1-σ standard deviation) of the T80 index and mesopause height is 5.0 K and 1.8 km, respectively, both of which are substantially larger than their respective long-term linear trends (2.5 K $decade^{-1}$ for T80 and 0.77 km $decade^{-1}$ for mesopause height). This demonstrates that interannual mesopause fluctuations predominate over slow long-term linear trends.

Figure 4 details the spatial structure of this relationship. Fig. 4(a) maps the latitude-by-latitude correlation coefficient (R) between the T80 index and the December mesopause height from 80°S to 50°N. The correlation is exceptionally strong and statistically significant (R > 0.85) throughout the high-latitude SH summer region from 80°S to 40°S, peaking at 0.98 near 60°S. The correlation weakens but remains significant at mid-latitudes before becoming statistically insignificant in the tropics. Intriguingly, weak yet statistically significant positive correlations emerge in the Northern subtropics, reaching ~0.65 near 10°N.

Fig. 4(b) reveals the T80–mesopause height linkage through the linear regression sensitivity (Δh/ΔT, in km K^{-1}) at varying latitudes. The sensitivity increases from 0.24 km K^{-1} at 80°S to a pronounced maximum of 0.50 km K^{-1} near 40°S—the latitude of the steepest gradient in the climatological mesopause height (see Fig. 1). The sensitivity then decreases sharply towards the subtropics and exhibits small, variable values in the Northern Hemisphere (NH), consistent with the weaker correlations shown in Fig. 4(a).

Figure 5 extends this analysis to November and January, during which SABER also observes the high latitudes of the winter hemisphere (53°N-83°N). The mesopause heights between 83ºS and 45°S remains significantly correlated with the T80 index in both months. In November and January, weak but significant positive correlations again appear near ~20°N, similar to the December pattern in Fig. 4. This positive correlation at low northern latitudes suggests a possible interhemispheric influence of the SH T80-driven upwelling on the NH mesopause.

https://doi.org/10.5194/egusphere-2026-3749
Preprint. Discussion started: 14 July 2026

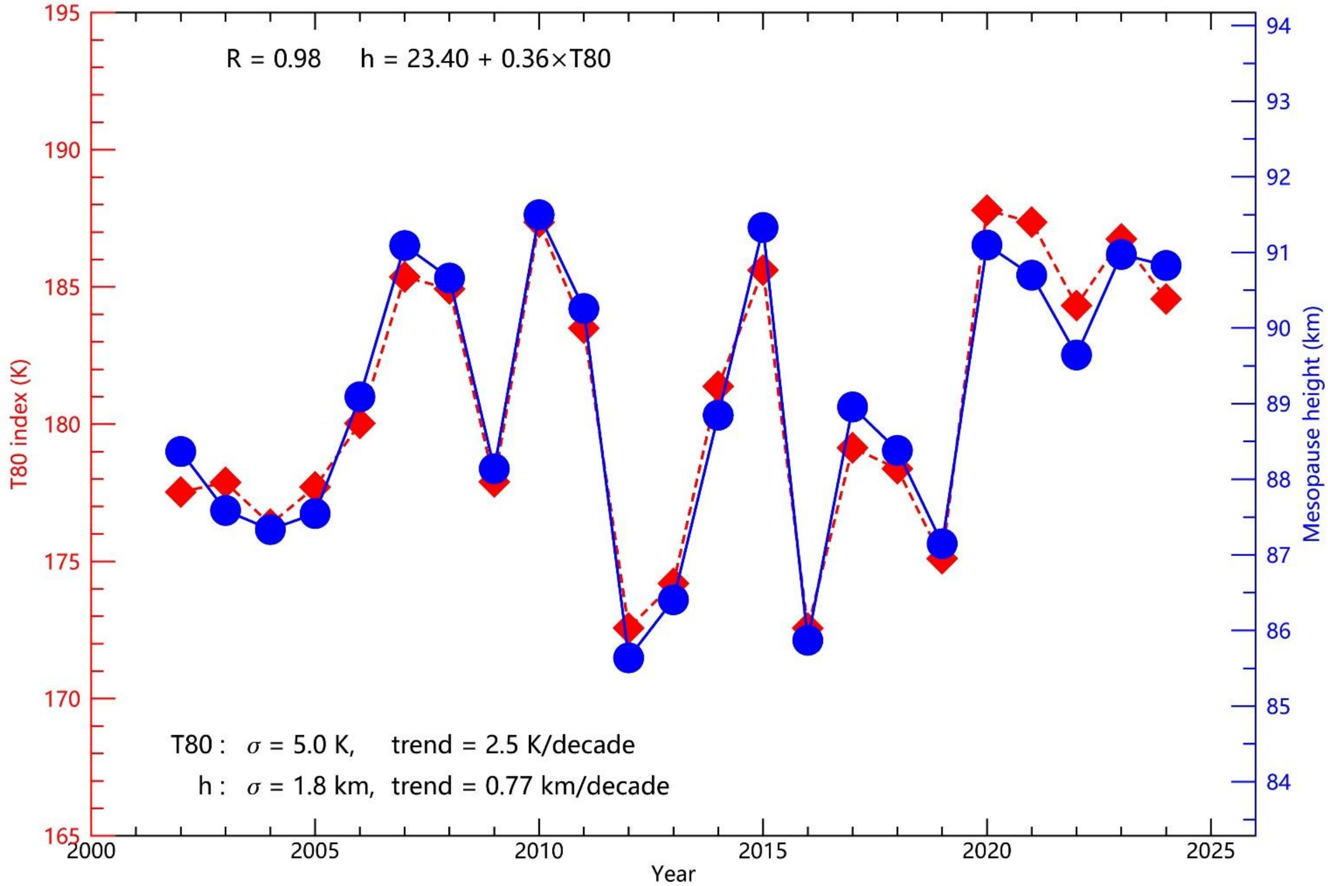

Figure 3. Dominant interannual control of the mesopause height by the T80 index at 60°S. The time series of the December T80 index (red) and the mesopause height at 60°S (blue) demonstrate near-perfect in-phase co-variability. The correlation coefficient (R), linear regression equation, interannual standard deviations (σ), and decadal linear trends for both variables are annotated.

https://doi.org/10.5194/egusphere-2026-3749
Preprint. Discussion started: 14 July 2026

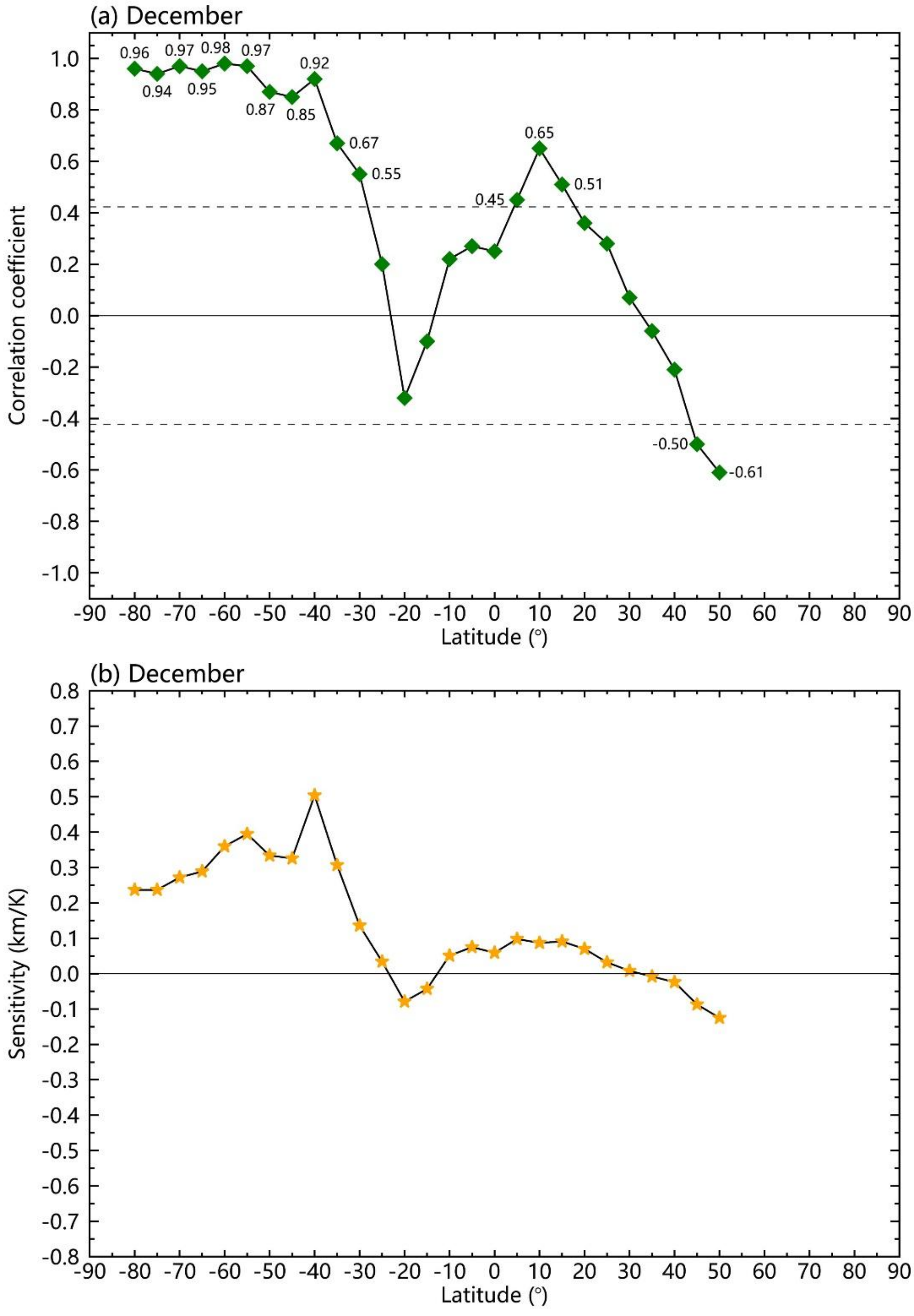

Figure 4. Latitudinal structure of the T80–mesopause height relationship in December. (a) the correlation coefficient and (b) the sensitivity between the T80 index and the mesopause height at varying latitudes from 80°S to 50°N. The horizontal dashed lines indicate the 0.95 significant level. The sensitivity is obtained by linear regression.

185

https://doi.org/10.5194/egusphere-2026-3749
Preprint. Discussion started: 14 July 2026

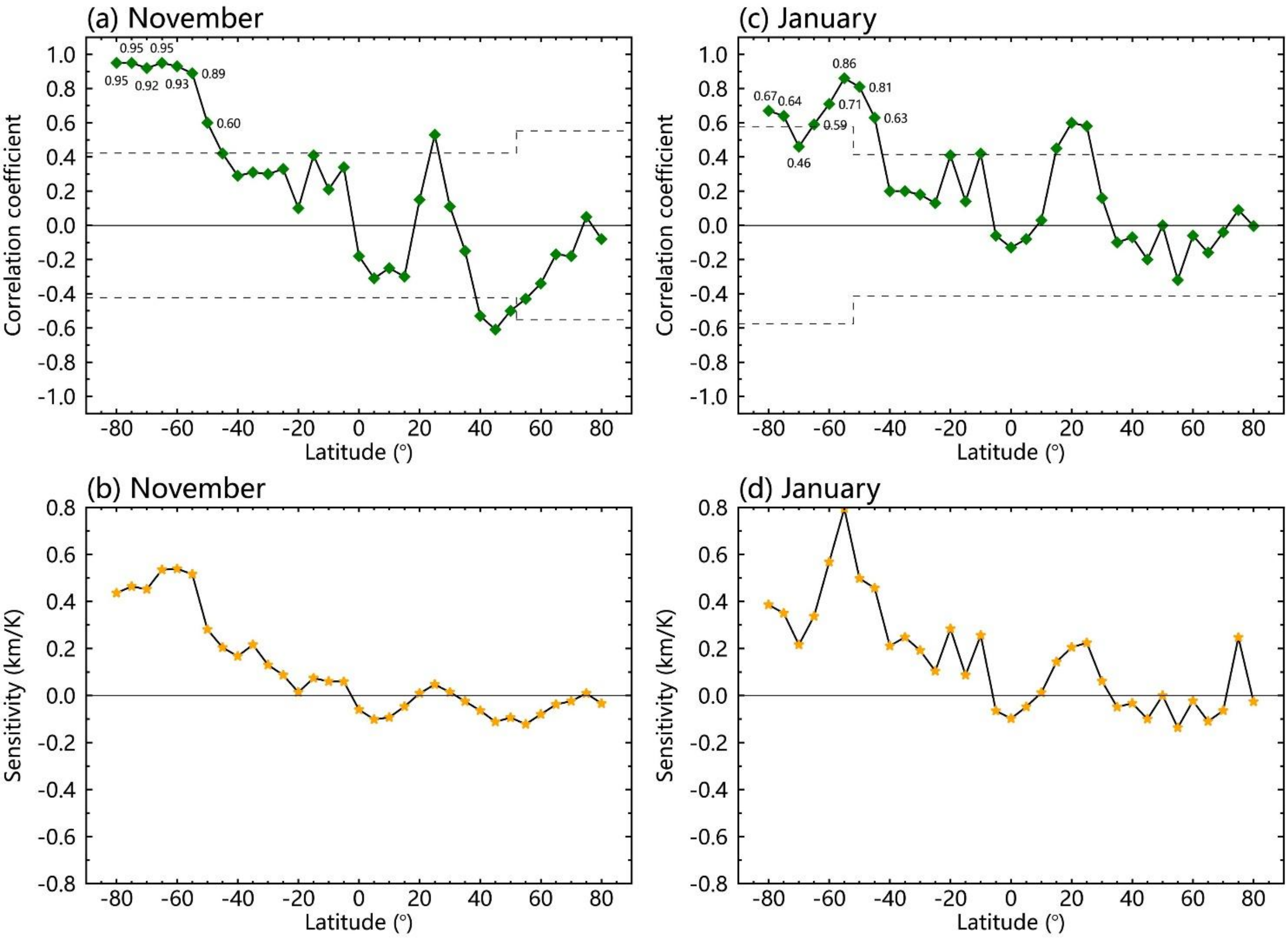

Figure 5. Relationship between the T80 index and mesopause height between 83°S and 83°N in (a-b) November and (c-d) January, similar to the correlation coefficients and the sensitivity in Fig. 4. The dashed lines are the 0.95 significant levels. Note that there are 13 years SABER observations between 53°N and 83°N in November, and 12 years SABER observations between 83°S and 53°S in January.

https://doi.org/10.5194/egusphere-2026-3749
Preprint. Discussion started: 14 July 2026

3.3 Statistical forecast for the mesopause height with one- or two-month lead

The strong month-to-month correlation of the T80 index (November-December R = 0.91; December–January R = 0.85), which reflects the persistent nature of the summer polar upwelling, provides a basis for forecasting the summer mesopause height with lead times of one or two months. Moreover, the high-latitude summer mesopause height itself exhibits strong month-to-month autocorrelation (at 60°S: November-December R = 0.85; December–January R = 0.89), likely arising from the inherent memory of the atmospheric system, which further favors predictability.

Figure 6(a) shows the correlation between the November T80 index and the December mesopause height across latitudes. Significant correlations are found between 80°S and 30°S, with coefficients up to 0.90 at 55°S and 40°S, and remaining above 0.80 across most latitudes from 80°S to 45°S. These results demonstrate that the November T80 index can serve as a skillful one-month-ahead predictor of the December mesopause height over a broad latitudinal range.

Fig. 6(b) extends the lead time to two months, showing the correlation between the November T80 index and the January mesopause height remains significant poleward of 45°S. Although the correlation coefficients are somewhat reduced compared to the one-month lead case, they remain statistically significant over the high-latitude region, indicating that the T80 index retains predictive skill even at a two-month lead time.

Fig. 6(c) shows the correlation between the December T80 index and the January mesopause height, representing a one-month lead from December to January. The correlations are comparable to those in Fig. 6(a), with values up to 0.87 at 60°S. Interestingly, the December T80–January mesopause height correlation is slightly stronger than the January T80–January mesopause height correlation (Fig. 5c). This likely occurs because interannual mesopause variations are more tightly linked to the December residual circulation state than concurrent January upwelling, which weakens as the solstice season progresses.

Taken together, these results establish that the T80 index provides a simple, observation-based tool for forecasting the summer high-latitude mesopause height with lead times of one to two months. The predictive skill stems from the high autocorrelation of both the T80 index and the mesopause height between consecutive months. This forecast capability represents, to our knowledge, the first demonstration of sub-seasonal to seasonal predictability for a key mesospheric parameter.

https://doi.org/10.5194/egusphere-2026-3749
Preprint. Discussion started: 14 July 2026

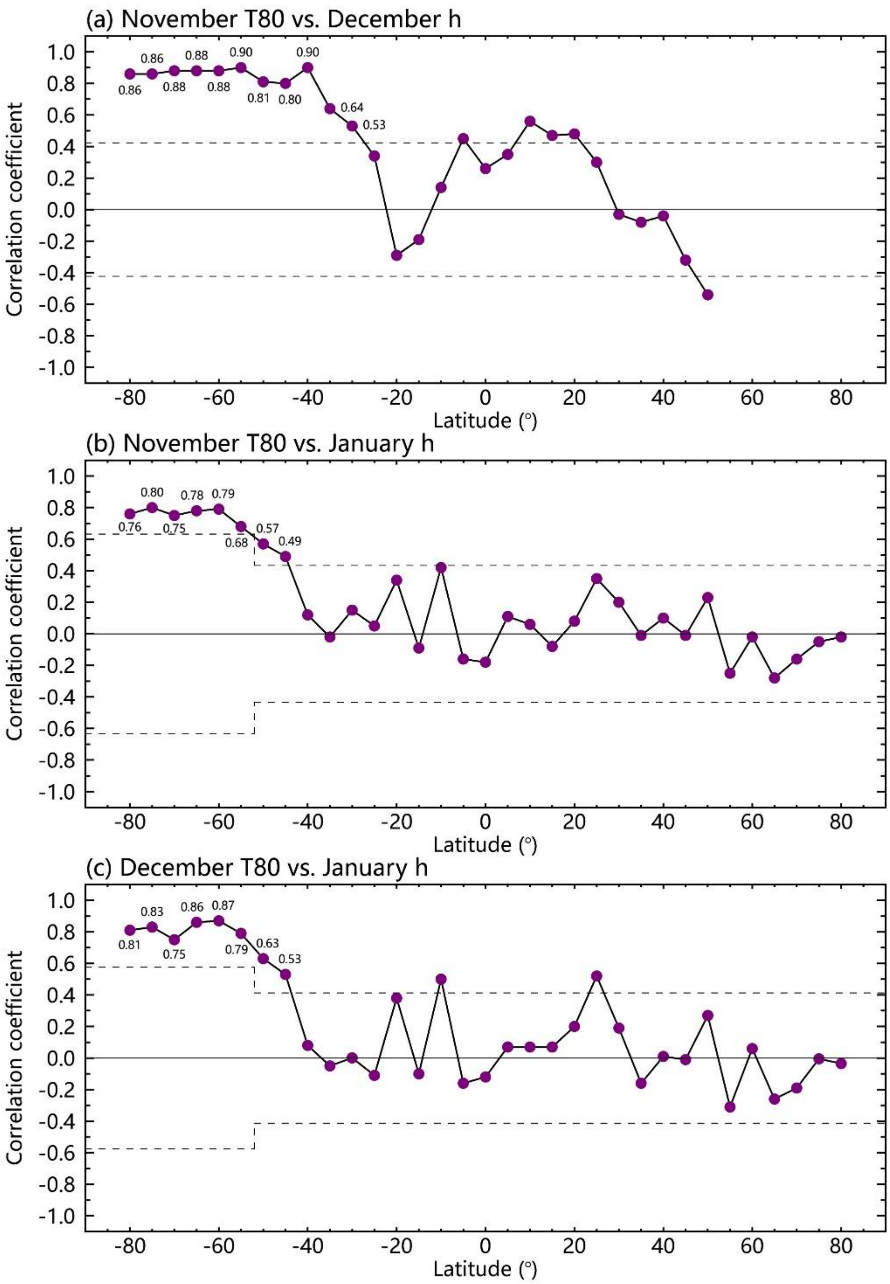

Figure 6. Correlation coefficients between the T80 upwelling index and the mesopause at varying latitudes with leading times of one or two months. (a) November T80 vs. December mesopause height. (b) November T80 vs. January mesopause height. (c) December T80 vs. January mesopause height. Dashed lines indicate the 95% significant level. Note that only 12 years of SABER observations are available between 53°S and 83°S in January.

https://doi.org/10.5194/egusphere-2026-3749
Preprint. Discussion started: 14 July 2026

3.4 The T80-mesopause linkage on daily scales

While the previous sections focused on interannual variability, here we examine whether the T80–mesopause height relationship holds on daily timescales. Figures 7 and 8 show the daily correlation at 60°S for each year from 2002 to 2025. Over the 24-year period, 19 years exhibit statistically significant correlations at the 95% confidence level, while 5 years do not. The insignificant years are 2004 (R = 0.22), 2014 (R = 0.11), 2016 (R = 0.12), 2020 (R = 0.09), and 2023 (R = −0.17), all falling below the significant threshold of R ≈ 0.26. The multi-year mean correlation coefficient is 0.48, and the mean sensitivity is 0.24 km K^{-1}.

As expected, the daily-scale correlations are lower than their interannual counterparts (R = 0.98 at 60°S), because daily variability includes transient wave events (gravity waves, tides, planetary waves) that introduce noise not present in the monthly averaged data. Nevertheless, the mean correlation of 0.48 indicates that the T80 index captures a substantial fraction of the daily mesopause height variability at high southern latitudes.

Figure 9 shows the latitudinal structure of the daily-scale relationship, averaged over all 24 years. Significant correlations are confined to latitudes poleward of 55°S (R ≈ 0.42–0.49), consistent with the interannual results. Between 50°S and 35°S, the correlations drop below the significant level, likely due to the strong dynamical variability in this midlatitude transition region. At latitudes north of 35°S, the correlations are negligible. The daily-scale sensitivity (Fig. 9b) shows a similar latitudinal pattern, with values of 0.20–0.30 km K^{-1} poleward of 55°S, decreasing rapidly toward the equator. This sensitivity is broadly consistent with the interannual sensitivity (0.36 km K^{-1} at 60°S).

In summary, the T80–mesopause height relationship is robust on daily timescales at high southern latitudes, albeit with lower correlation coefficients than on interannual timescales due to the presence of transient wave noise. The consistency between daily and interannual sensitivities supports the interpretation that the same underlying mechanism governs the mesopause height variability across timescales.

https://doi.org/10.5194/egusphere-2026-3749
Preprint. Discussion started: 14 July 2026

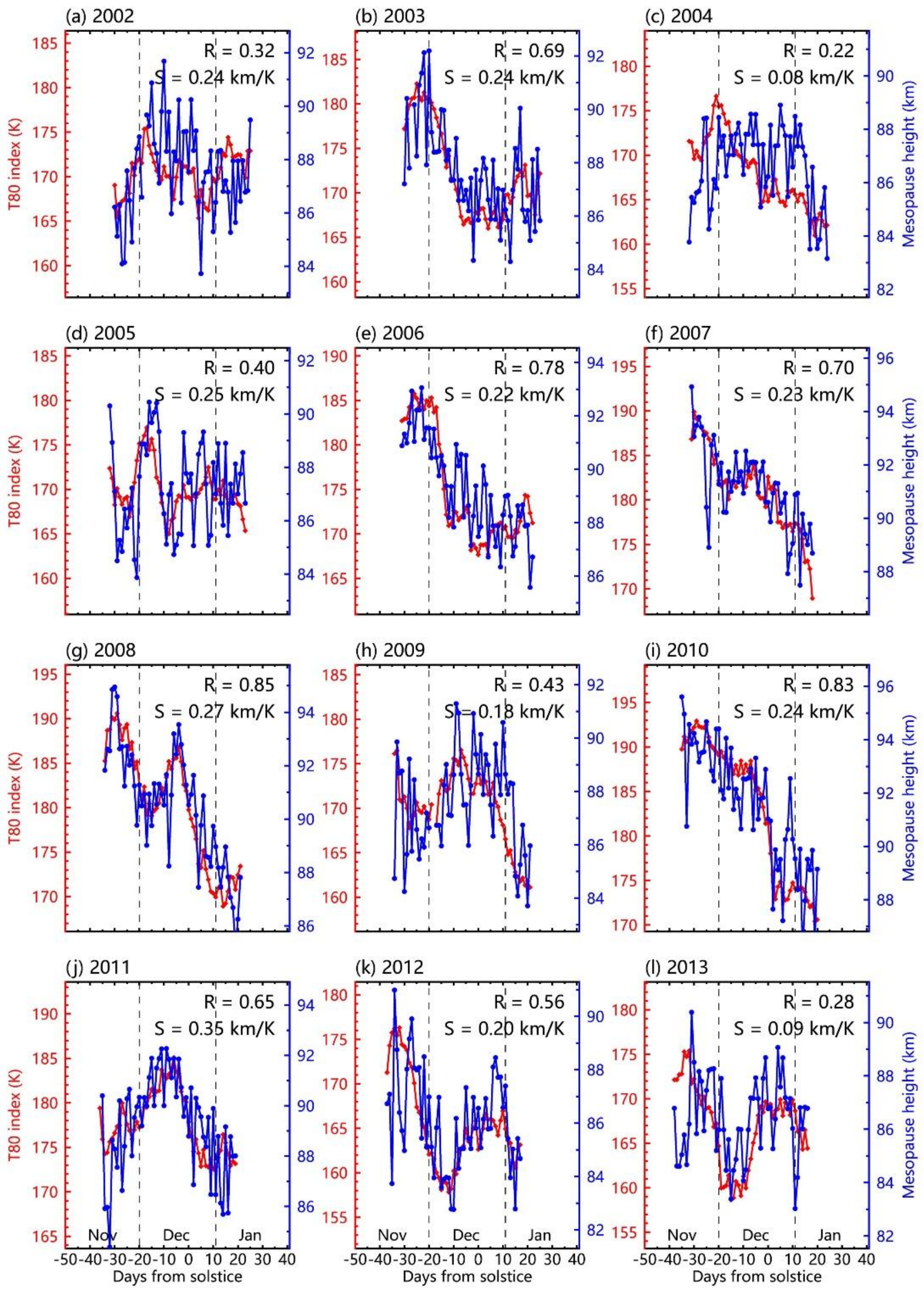

Figure 7. Daily-scale relationship between the T80 index and mesopause height at 60°S for each year from 2002 to 2013. The T80 index is the zonal and daily mean SABER temperature between 75°S and 83°S at ~80 km. Approximately 56 days of SABER data are available each summer at high latitudes. The dashed line indicates the 95% significant level (R ≈ 0.26); only the correlation in 2004 (R = 0.22) falls below this threshold.

https://doi.org/10.5194/egusphere-2026-3749
Preprint. Discussion started: 14 July 2026

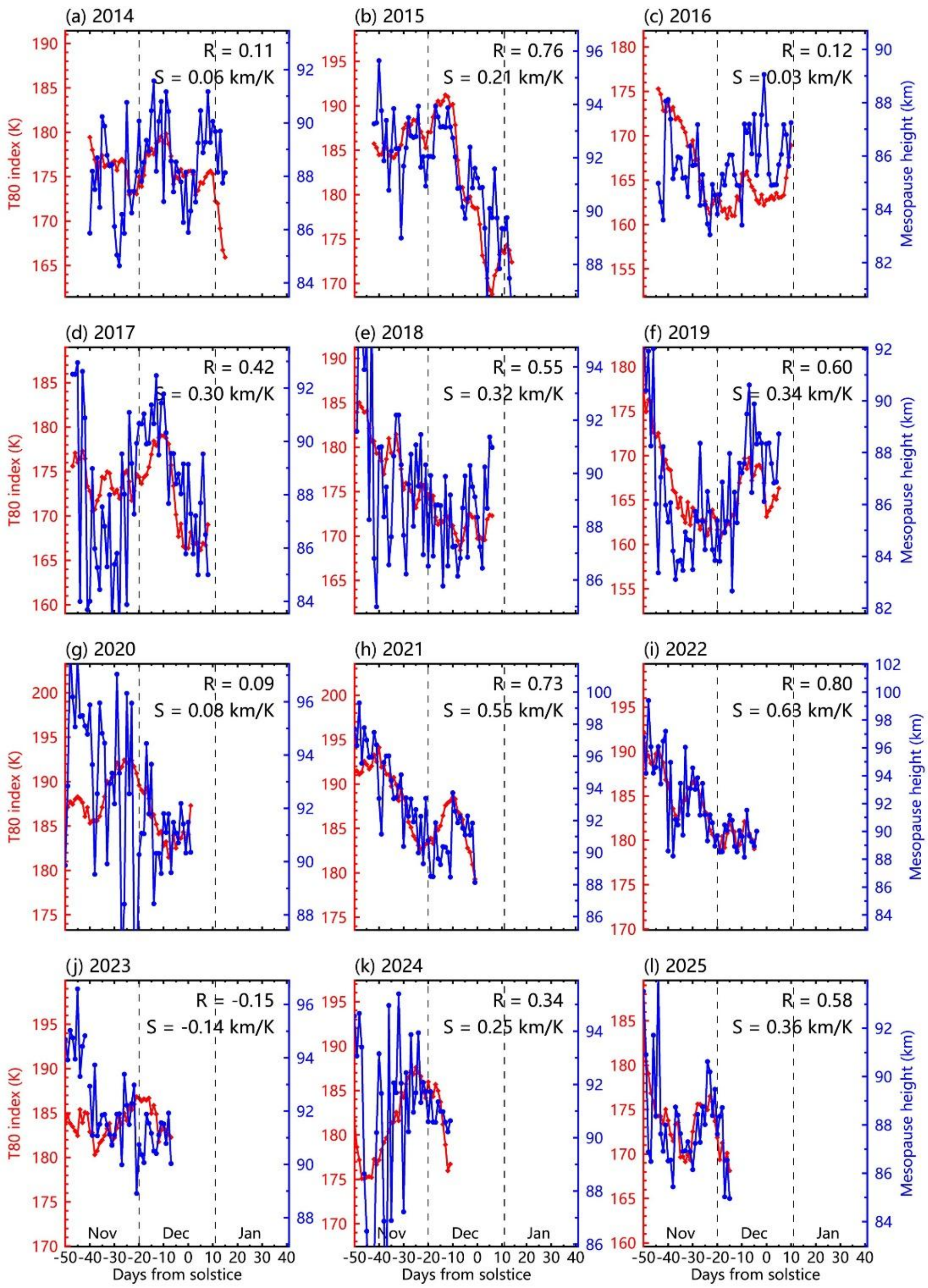

Figure 8. Same as Fig. 7, but for the years 2014 to 2025. The correlations in 2014 (R = 0.11), 2016 (R = 0.12), 2020 (R = 0.09), and 2023 (R = −0.15) do not exceed the 95% significant level.

https://doi.org/10.5194/egusphere-2026-3749
Preprint. Discussion started: 14 July 2026

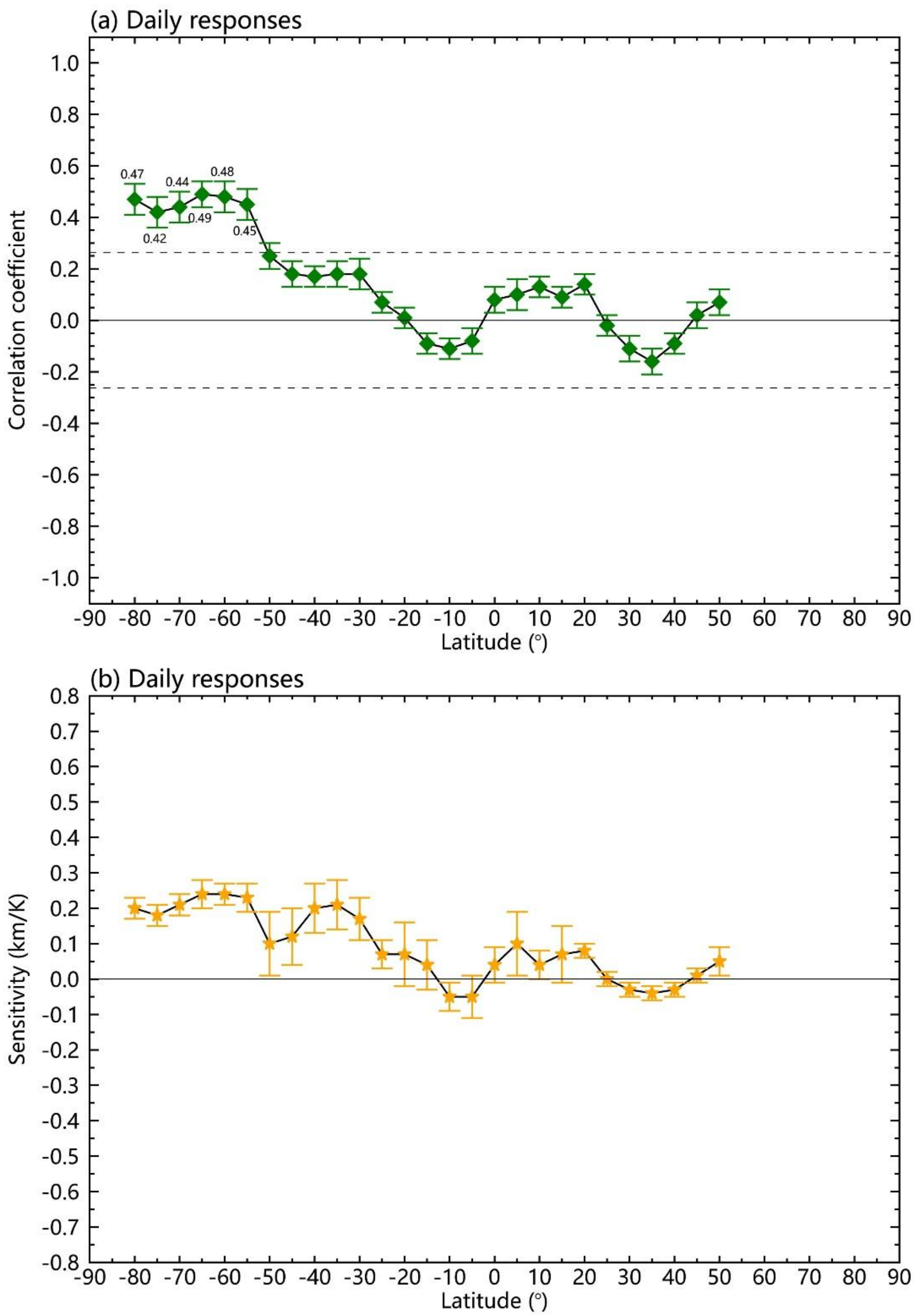

255 **Figure 9.** Latitudinal structure of the daily-scale T80–mesopause height relationship, averaged over 2002–2025. (a) Mean correlation coefficient and (b) mean sensitivity (km K^{-1}) between the T80 index and mesopause height from 80°S to 50°N. Error bars denote the standard deviation of the 24 annual values. The horizontal dashed line indicates the 95% significant level.

https://doi.org/10.5194/egusphere-2026-3749
Preprint. Discussion started: 14 July 2026

4 Discussion

4.1 Mechanism: vertical dipole temperature response to the T80 index

The T80 index controls the mesopause height variability through a vertical dipole temperature response to the summer polar upwelling fluctuations, involving coupled dynamical, microphysical, chemical, and thermal processes.

Figure 10a shows the correlation and sensitivity between the T80 index and temperatures at 60°S from 80 to 103 km in December on interannual timescales. Below ~90 km, temperatures are positively correlated with the T80 index, consistent with adiabatic cooling during stronger upwelling (i.e., a lower T80 index corresponds to colder temperatures below 90 km), peaking at 84 km with R = 0.97. Above ~90 km, the correlation reverses sign and becomes strongly negative, peaking at 95 km with R = −0.96. This reversal is the hallmark of the bottom-up mechanism, which operates through the following chain: Stronger summer polar upwelling → lower temperature below 90 km (lower T80) → enhanced growth of PMC ice particles → cold-trap effect dehydrates the region above the PMC layer → reduced H_2O leads to increased O_3 and O → enhanced chemical and radiative heating raises temperatures above 90 km (*Zhang et al.*, 2025c).

The sensitivity of temperature to the T80 index (blue curve in Fig. 10a) mirrors the correlation pattern. Below 90 km, the sensitivity is positive (peaking at 84 km with 0.88 K K^{-1}), while above 90 km it is negative (peaking at 95 km with −1.47 K K^{-1}). The crossover point at ~90 km coincides closely with the climatological mesopause height at this latitude.

Figs. 10b and 10c illustrate how this dipole response translates into vertical displacement of the mesopause. For a T80 decrease of -5 K (Fig. 10b), representing stronger upwelling, the temperature below 90 km cools and the temperature above 90 km warms. The net effect is a downward shift of the entire temperature profile near the mesopause, lowering the mesopause height from ~89 km to ~87 km. Conversely, for a T80 increase of +5 K (Fig. 10c), representing weaker upwelling, the opposite occurs: the temperature below 90 km warms and above 90 km cools, raising the mesopause height from ~89 km to ~91 km. The vertical displacement of the mesopause is approximately proportional to the T80 change, consistent with the observed sensitivity of 0.36 km K^{-1} at 60°S (Fig. 3).

A critical aspect of this mechanism is that the turning point of the temperature sensitivity (near 90 km) is located very close to the climatological mesopause height. If the turning point were situated substantially higher or lower than the mesopause, the temperature profile near the mesopause would warm or cool uniformly, and the mesopause height would exhibit little change. We will revisit this argument in the next section to explain why solar activity also does not affect the mesopause height.

In summary, the dipole temperature response—cooling below and warming above 90 km—quantitatively account for the T80-induced shift of the mesopause height, linking large- scale upwelling dynamics to the vertical thermal structure through coupled dynamical- microphysical- chemical-thermal processes.

https://doi.org/10.5194/egusphere-2026-3749
Preprint. Discussion started: 14 July 2026

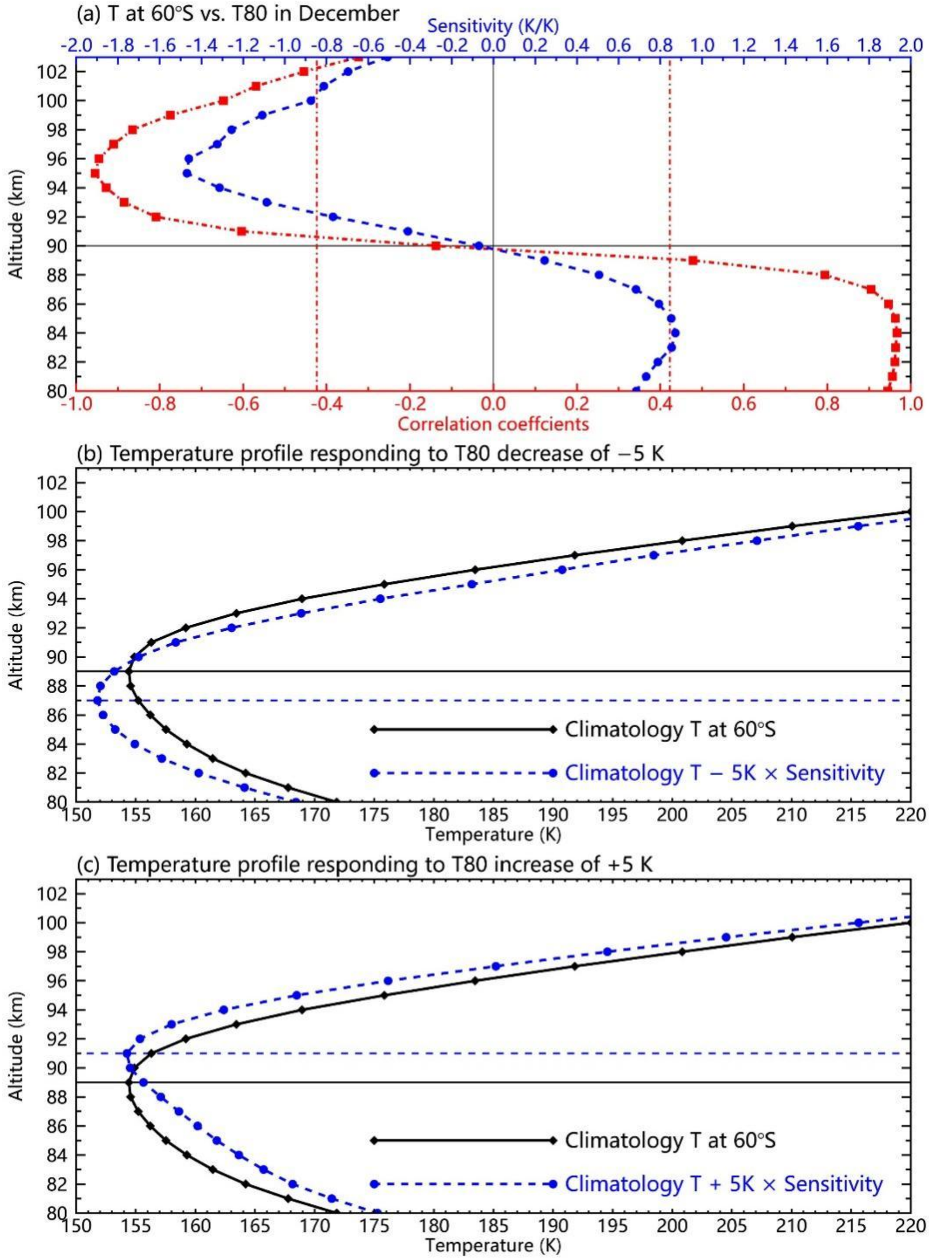

290 **Figure 10.** Mechanism of the T80 upwelling index modulating the mesopause height at 60°S in December on interannual timescales. (a) Correlation coefficients (red) and sensitivity (blue) of temperatures at varying altitudes to the T80 index. Dashed lines mark the 95% significant level for the correlation coefficients. (b) Comparison between the climatological temperature profile (solid) and the profile corresponding to a T80 decrease of -5 K (dashed). The mesopause heights of the two profiles are indicated by horizontal lines. (c) Same as (b), but for a T80 increase of +5 K.

https://doi.org/10.5194/egusphere-2026-3749
Preprint. Discussion started: 14 July 2026

4.2 The detectability of solar and CO_2 signals in mesopause height

As demonstrated above, the T80 index dominates interannual variations of summer mesopause height. We now examine whether external forcings (the 11-year solar cycle and long-term CO_2 cooling) can be detected in the current 24-year record.

The solar radiation flux at 10.7 cm (f10.7, in units of sfu = 10^{-22} Wm^{-2} Hz^{-1}) is applied to represent solar activity (*Tapping*, 2013). Figure 11a shows that the December T80 index and f10.7 are essentially uncorrelated (R = 0.16), confirming that the summer polar upwelling is not modulated by the solar cycle. Consequently, in the high-latitude summer region (80°S–40°S), where the T80 index dominates the thermal structure, solar f10.7 has no significant influence on either the mesopause temperature or the mesopause height (Fig. 11b and 11c).

At lower latitudes (40°S–50°N), where the mesopause resides at higher altitudes (~98 km), a different situation emerges. Solar f10.7 does affect the mesopause temperature (Fig. 11c), with positive correlations of 0.73 at 98 km. However, it does not affect the mesopause height (Fig. 11b). The reason is illustrated in Fig. 11d and 11e, using 10°S as an example. Fig. 11d shows the correlation and sensitivity of temperatures at varying altitudes to f10.7. Critically, both above and below the mesopause height (~98 km), the correlations and sensitivities are positive, indicating that solar radiative heating produces vertically coherent warming across the full temperature profile. Fig. 11e compares the climatological temperature profile at 10°S with the profile for a 100 sfu increase in f10.7. As expected, the temperature profile shifts uniformly, but the cold-point mesopause height remains unchanged (at 98 km). This is the same logic introduced in Section 4.1: if the temperature profile warms or cools uniformly, the mesopause height does not move.

In summary, within the current 24-year record, solar activity has no detectable effect on mesopause height at any latitude. At high latitudes, the solar signal is masked by T80-driven dynamical variability. At mid- and low latitudes, solar heating affects the mesopause temperature but not its height, because the heating is vertically uniform. However, we note that robust detection of a solar cycle signal in the mesopause likely requires at least three solar cycles (~33 years) of continuous observations to separate it from dynamical effects.

Rising atmospheric CO_2 induces radiative cooling and gradual contraction of the mesosphere, which should lower the mesopause height. Figure 12 compares the interannual variability and the linear trend of mesopause height and temperature in December across latitudes. The interannual standard deviations of mesopause height and temperature are substantially larger than their linear trends. The results for November and January are similar and are not shown.

We emphasize that this does not contradict the well-established role of CO_2 in driving long-term mesospheric cooling and contraction. Rather, it demonstrates that on interannual timescales and within the current 24-year record, the variability of the summer mesopause height is overwhelmingly dominated by internal dynamical forcing—specifically, the strength of the summer polar upwelling. Robust detection of the CO_2-driven contraction trend in the summer mesopause will likely require longer observational records and careful separation from dynamical and solar cycle contributions.

https://doi.org/10.5194/egusphere-2026-3749
Preprint. Discussion started: 14 July 2026

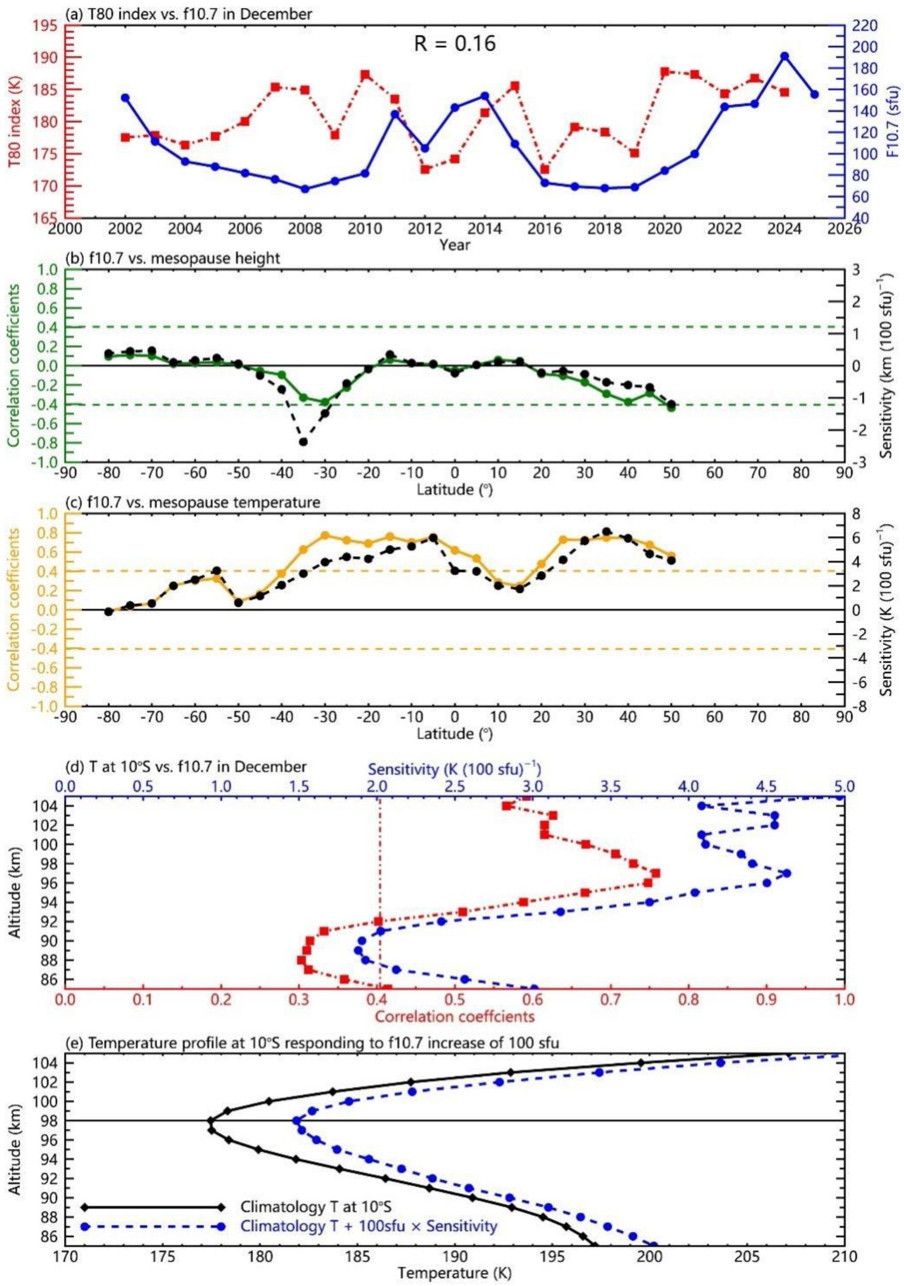

Figure 11. Influence of solar 11-year activity on mesopause height and temperature. (a) The T80 index in December is uncorrelated with solar f10.7 flux. (b, c) Correlation between f10.7 and mesopause height/temperature at varying latitudes. (d) Correlation coefficients (red) and sensitivity (blue) of temperatures at 10°S to solar f10.7 at varying altitudes. (e) Climatological temperature profile at 10°S (solid) and the profile corresponding to a 100 sfu increase in f10.7 (dashed). Dashed lines in (b–c) indicate the 95% significant level. Sensitivities are calculated by linear regression.

https://doi.org/10.5194/egusphere-2026-3749
Preprint. Discussion started: 14 July 2026

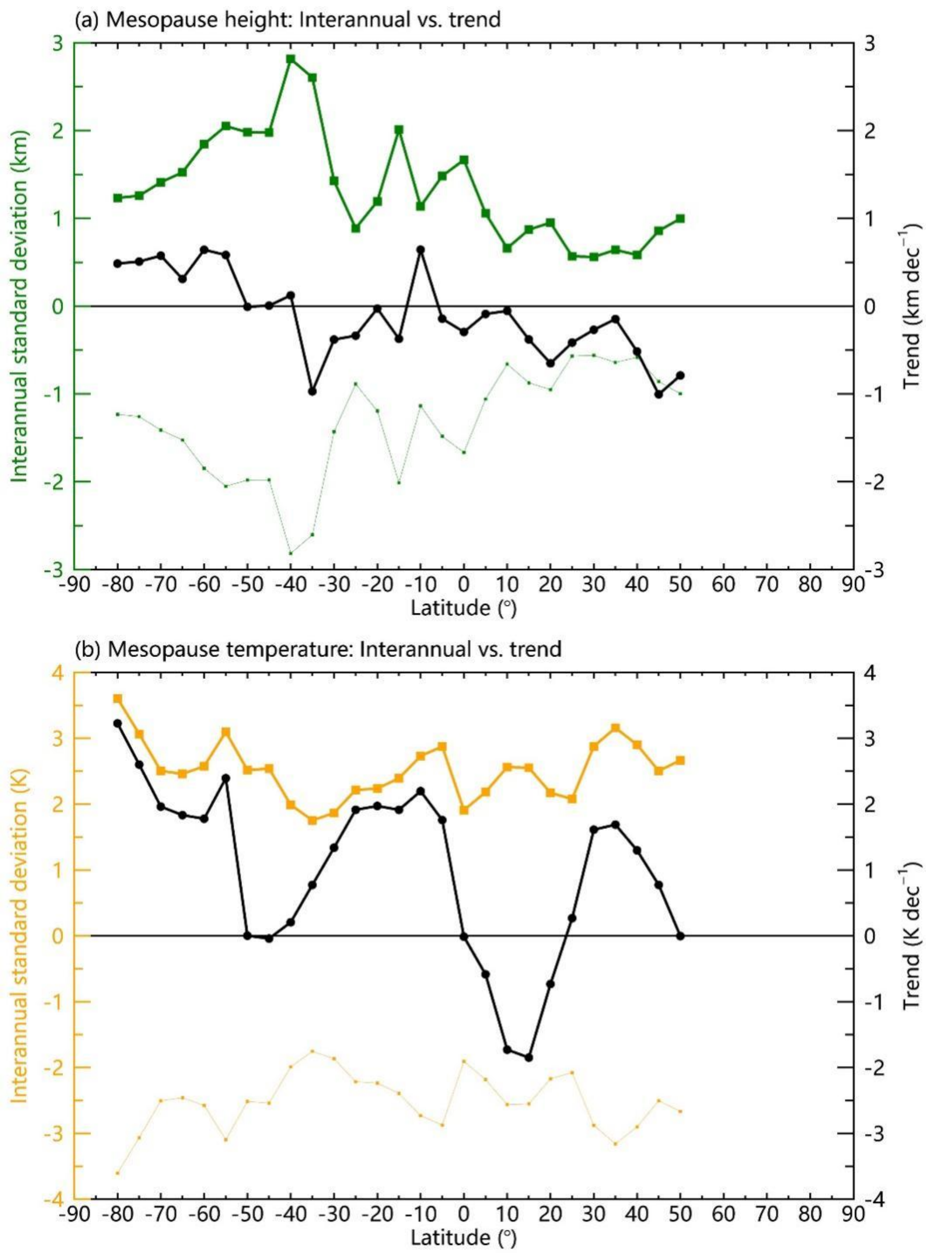

Figure 12. Comparison of interannual variability and long-term trend for (a) mesopause height and (b) mesopause temperature at varying latitudes in December. The interannual variability is substantially larger than the long-term linear
335 trend, indicating that the CO_2-driven cooling is masked by internal dynamical variability in December.

https://doi.org/10.5194/egusphere-2026-3749
Preprint. Discussion started: 14 July 2026

4.3 Limitations and open questions

Several limitations and open questions should be acknowledged. Our analysis is restricted to the SH summer months (November–January). For the NH summer months (May–July), our preliminary analysis suggests a similar but interhemispherically asymmetric relationship, which will be further explored in a separate paper.

The T80–mesopause height correlation on daily timescales (Figs. 7–8) is statistically insignificant in 5 out of 24 years (2004, 2014, 2016, 2020, and 2023). Notably, some of these years coincide with strong solar transient activity, which may affect mesopause temperature (*Becker and von Savigny*, 2010; *Enengl et al.*, 2021; *Huang et al.*, 2025; *Sun et al.*, 2025; *Zou et al.*, 2020). The underlying physical mechanisms require further investigation, but are beyond the scope of the present paper.

Moreover, a notable feature in our results is the weak but statistically significant correlation between T80 index and the mesopause height at low latitudes in the NH (Figs. 4 and 5). This positive correlation suggests that the T80-driven summer polar upwelling in the SH may exert a remote influence on the NH mesopause via the cross-equatorial transport of H_2O and associated chemical/thermal perturbations (*Zhang et al.*, 2025c). However, the detailed mechanism remains unclear.

The linkage between T80-modulated mesopause height and associated phenomena, such as PMCs, airglow, and metal layers, deserves follow-up studies. For example, since PMC peak altitude is typically 3–4 km below the mesopause (*Russell III et al.*, 2010), a T80-driven change in mesopause height should be accompanied by a corresponding shift in PMC altitude.

Previous studies have attributed the absence of solar signals in the summer polar mesopause temperature to a compensating dynamical cooling effect (*Karlsson and Kuilman*, 2018; *Qian et al.*, 2019). Our results offer an alternative explanation: the T80 index dominates the interannual variability, and the solar signal is simply too weak to be detected against this dynamical background.

The CO_2-driven cooling trend in the mesopause height during December is not yet separable from the dominant interannual variability within the current 24-year record. Although the role of CO_2 in driving long-term mesospheric contraction is well-established and widely recognized, extracting this signal during summer months requires longer observational records (multiple decades) and careful separation of the radiative contribution (solar f10.7 and CO_2) from the dynamical contribution (T80 index). The present 24-year window is insufficient for this purpose.

5 Conclusion

Using 24 years (2002–2025) of SABER temperature measurements, this study demonstrates that the summer mesopause height in the SH is almost perfectly controlled by the T80 index—a temperature-based proxy for the strength of summer polar upwelling. The key findings are summarized as follows.

On interannual timescales, the T80 index dominates the December mesopause height variability across 30°S–80°S, with a correlation coefficient of 0.98 and sensitivity of 0.36 km K^{-1} at 60°S. This relationship holds robustly for all

https://doi.org/10.5194/egusphere-2026-3749
Preprint. Discussion started: 14 July 2026

individual months from November to January. On daily timescales, the T80-mesopause height correlation remains significant but is largely confined to latitudes poleward of 55°S. In the mid-latitude transition region, the daily relationship weakens, likely due to the stronger daily perturbations of mesopause height.

The underlying mechanism involves the dipole temperature response to T80 index: stronger upwelling (lower T80) produces adiabatic cooling below ~90 km and chemical/radiative heating above ~90 km. This opposing response arises from a chain of dynamical, microphysical (i.e., the PMC cold-trap effect), ozone chemical, and thermal processes (*Zhang et al.*, 2025c). The resulting downward shift of the entire temperature profile physically lowers the mesopause height.

The strong month-to-month persistence of both the T80 index and mesopause temperatures provides a practical basis for forecasting. Specifically, the November T80 index predicts the December mesopause height with a correlation coefficient up to 0.90, offering a one-month-ahead statistical prediction capability.

Signals of the 11-year solar cycle and multi-decadal CO_2 radiative cooling cannot be robustly separated from dominant internal dynamical variability within the 24-year SABER record. Longer observational records are needed to robustly extract these external forcing signals.

Taken together, these results establish the T80 index as a powerful diagnostic and predictive tool for understanding and forecasting the state of the mesopause region. The near-perfect control of mesopause height by internal dynamics, alongside the difficulty in detecting external forcing signals within a 24-year record, highlights the need to incorporate bottom-up dynamical–microphysical–chemical–thermal coupling into future models of the mesosphere and lower thermosphere.

Data Availability. The MLS Level 2, version 5 data are available for download from the NASA GES DISC website, with the temperature data accessible at https://disc.gsfc.nasa.gov/datasets/ML2T_005/summary. The quality document of MLS is available at https://mls.jpl.nasa.gov/data/v5-0_data_quality_document.pdf. The SABER data version 2.07 of temperature can be downloaded from https://data.gats-inc.com/saber/custom/Temp_O3_H2O/v2.0/. The solar f10.7 data can be obtained at https://omniweb.gsfc.nasa.gov/form/dx1.html via the GSFC/SPDF OMNI web interface.

Author Contributions. Liang Zhang conceived the idea, analyzed the data, and drafted the manuscript. Zhongfang Liu revised the paper. Yajun Zhu revised the paper.

Competing Interests. The authors declare that they have no conflict of interests.

Acknowledgements. We are especially grateful to the MLS and SABER program for providing us with the long-range and high-quality data, and we further wish to acknowledge the OMNI group for providing high-quality solar f10.7 data. We also

https://doi.org/10.5194/egusphere-2026-3749
Preprint. Discussion started: 14 July 2026

thank Dr. Zheng Sheng for his valuable suggestions.

Financial support. This research has been supported by the National Natural Science Foundation of China (42025602 and 41905059).

References

Becker, E. and von Savigny, C. (2010), Dynamical heating of the polar summer mesopause induced by solar proton events, *Journal of Geophysical Research: Atmospheres*, *115*(D1), https://doi.org/10.1029/2009JD012561.

Enengl, F., Partamies, N., Ivchenko, N. and Baddeley, L. (2021), On the relationship of energetic particle precipitation and mesopause temperature, *Ann. Geophys.*, *39*(5), 795-809, https://doi.org/10.5194/angeo-39-795-2021.

García-Comas, M., Funke, B., Gardini, A., López-Puertas, M., Jurado-Navarro, A., von Clarmann, T., Stiller, G., Kiefer, M., Boone, C. D., Leblanc, T., Marshall, B. T., Schwartz, M. J. and Sheese, P. E. (2014), MIPAS temperature from the stratosphere to the lower thermosphere: Comparison of vM21 with ACE-FTS, MLS, OSIRIS, SABER, SOFIE and lidar measurements, *Atmos. Meas. Tech.*, *7*(11), 3633-3651, https://doi.org/10.5194/amt-7-3633-2014.

Garcia, R. R. and Solomon, S. (1985), The effect of breaking gravity waves on the dynamics and chemical composition of the mesosphere and lower thermosphere, *Journal of Geophysical Research: Atmospheres*, *90*(D2), 3850-3868, https://doi.org/10.1029/JD090iD02p03850.

Holton, J. R. (1983), The Influence of Gravity Wave Breaking on the General Circulation of the Middle Atmosphere, *Journal of Atmospheric Sciences*, *40*(10), 2497-2507, https://doi.org/10.1175/1520-0469(1983)040<2497:TIOGWB>2.0.CO;2.

Huang, N., Li, J., Lu, J., Fu, S., Sun, M., Wei, G., Zhan, M., Wang, M. and Xiong, S. (2025), Mesosphere and Lower Thermosphere (MLT) Density Responses to the May 2024 Superstorm at Mid-to-High Latitudes in the Northern Hemisphere Based on Sounding of the Atmosphere Using Broadband Emission Radiometry (SABER) Observations, in *Remote Sensing*, edited, p. 511, https://doi.org/10.3390/rs17030511.

Jiang, Y. B., Froidevaux, L., Lambert, A., Livesey, N. J., Read, W. G., Waters, J. W., Bojkov, B., Leblanc, T., McDermid, I. S., Godin-Beekmann, S., Filipiak, M. J., Harwood, R. S., Fuller, R. A., Daffer, W. H., Drouin, B. J., Cofield, R. E., Cuddy, D. T., Jarnot, R. F., Knosp, B. W., Perun, V. S., Schwartz, M. J., Snyder, W. V., Stek, P. C., Thurstans, R. P., Wagner, P. A., Allaart, M., Andersen, S. B., Bodeker, G., Calpini, B., Claude, H., Coetzee, G., Davies, J., De Backer, H., Dier, H., Fujiwara, M., Johnson, B., Kelder, H., Leme, N. P., König-Langlo, G., Kyro, E., Laneve, G., Fook, L. S., Merrill, J., Morris, G., Newchurch, M., Oltmans, S., Parrondos, M. C., Posny, F., Schmidlin, F., Skrivankova, P., Stubi, R., Tarasick, D., Thompson, A., Thouret, V., Viatte, P., Vömel, H., von Der Gathen, P., Yela, M. and Zablocki, G. (2007), Validation of Aura Microwave Limb Sounder Ozone by ozonesonde and lidar measurements, *Journal of Geophysical Research: Atmospheres*, *112*(D24), https://doi.org/10.1029/2007JD008776.

Karlsson, B. and Kuilman, M. (2018), On How the Middle Atmospheric Residual Circulation Responds to the Solar Cycle Close to the Solstices, *Journal of Climate*, *31*(1), 401-421, https://doi.org/10.1175/JCLI-D-17-0202.1.

Li, Y., Gao, H., Sun, S. and Li, X. (2024), Correlation between Peak Height of Polar Mesospheric Clouds and Mesopause Temperature, in *Atmosphere*, edited, https://doi.org/10.3390/atmos15101149.

Lindzen, R. S. (1981), Turbulence and stress owing to gravity wave and tidal breakdown, *Journal of Geophysical Research*, *86*(C10), 9707-9714, https://doi.org/10.1029/JC086iC10p09707.

Liu, X., Xu, J., Yue, J., Yuan, T., She, C. Y. and Vital, L. F. R. (2026), Assessments the Long-Term Stability of the SABER Temperature Measurement in the Middle Latitude MLT Region, *Journal of Geophysical Research: Space Physics*, *131*(4), e2025JA034476, https://doi.org/10.1029/2025JA034476.

Plane, J. M. C., Gardner, C. S., Yu, J., She, C. Y., Garcia, R. R. and Pumphrey, H. C. (1999), Mesospheric Na layer at 40°N: Modeling and observations, *Journal of Geophysical Research: Atmospheres*, *104*(D3), 3773-3788, https://doi.org/10.1029/1998JD100015.

Plane, J. M. C., Gumbel, J., Kalogerakis, K. S., Marsh, D. R. and von Savigny, C. (2023), Opinion: Recent developments and future directions in studying the mesosphere and lower thermosphere, *Atmospheric Chemistry and Physics*, *23*(20), 13255-13282, https://doi.org/10.5194/acp-23-13255-2023.

Pramitha, M., Praveen, M. and Ratnam, M. V. (2025), Mesopause Insights: Unraveling Temperature and Height Trends Through SABER/TIMED and SD WACCM X Simulations, *Journal of Geophysical Research: Space Physics*, *130*(6), e2024JA033457, https://doi.org/10.1029/2024JA033457.

Qian, L., Jacobi, C. and McInerney, J. (2019), Trends and Solar Irradiance Effects in the Mesosphere, *Journal of Geophysical Research: Space Physics*, *124*(2), 1343-1360, https://doi.org/10.1029/2018JA026367.

Remsberg, E. E., Marshall, B. T., Garcia-Comas, M., Krueger, D., Lingenfelser, G. S., Martin-Torres, J., Mlynczak, M. G., Russell Iii, J. M., Smith, A. K., Zhao, Y., Brown, C., Gordley, L. L., Lopez-Gonzalez, M. J., Lopez-Puertas, M., She, C. Y., Taylor, M. J. and Thompson, R. E. (2008), Assessment of the quality of the Version 1.07 temperature-versus-pressure profiles of the middle atmosphere from TIMED/SABER, *Journal of Geophysical Research: Atmospheres*, *113*(D17), https://doi.org/10.1029/2008JD010013.

Russell III, J. M., Rong, P., Bailey, S. M., Hervig, M. E. and Petelina, S. V. (2010), Relationship between the summer mesopause and polar mesospheric cloud heights, *Journal of Geophysical Research: Atmospheres*, *115*(D16), https://doi.org/10.1029/2010JD013852.

Russell, J., Mlynczak, M., Gordley, L., Tansock, J. and Esplin, R. (1999), Overview of the SABER experiment and preliminary calibration results, *SPIE Proceedings*, *3756*(20), 277-288, https://doi.org/10.1117/12.366382.

Schwartz, M. J., Lambert, A., Manney, G. L., Read, W. G., Livesey, N. J., Froidevaux, L., Ao, C. O., Bernath, P. F., Boone, C. D., Cofield, R. E., Daffer, W. H., Drouin, B. J., Fetzer, E. J., Fuller, R. A., Jarnot, R. F., Jiang, J. H., Jiang, Y. B., Knosp, B. W., Krüger, K., Li, J. L. F., Mlynczak, M. G., Pawson, S., Russell Iii, J. M., Santee, M. L., Snyder, W. V., Stek, P. C., Thurstans, R. P., Tompkins, A. M., Wagner, P. A., Walker, K. A., Waters, J. W. and Wu, D. L. (2008), Validation of the Aura Microwave Limb Sounder temperature and geopotential height measurements, *Journal of Geophysical Research: Atmospheres*, *113*(D15), https://doi.org/10.1029/2007JD008783.

She, C.-Y., Berger, U., Yan, Z.-A., Yuan, T., Lübken, F. J., Krueger, D. A. and Hu, X. (2019), Solar Response and Long-Term Trend of Midlatitude Mesopause Region Temperature Based on 28 Years (1990–2017) of Na Lidar Observations, *Journal of Geophysical Research: Space Physics*, *124*(8), 7140-7156, https://doi.org/10.1029/2019JA026759.

She, C. Y. and von Zahn, U. (1998), Concept of a two-level mesopause: Support through new lidar observations, *Journal of Geophysical Research: Atmospheres*, *103*(D5), 5855-5863, https://doi.org/10.1029/97JD03450.

Sheese, P. E., Llewellyn, E. J., Gattinger, R. L., Bourassa, A. E., Degenstein, D. A., Lloyd, N. D. and McDade, I. C. (2011), Mesopause temperatures during the polar mesospheric cloud season, *Geophysical Research Letters*, *38*(11), https://doi.org/10.1029/2011GL047437.

Siskind, D. E., Drob, D. P., Emmert, J. T., Stevens, M. H., Sheese, P. E., Llewellyn, E. J., Hervig, M. E., Niciejewski, R. and Kochenash, A. J. (2012), Linkages between the cold summer mesopause and thermospheric zonal mean circulation, *Geophysical Research Letters*, *39*(1), https://doi.org/10.1029/2011GL050196.

Siskind, D. E., Merkel, A. W., Marsh, D. R., Randall, C. E., Hervig, M. E., Mlynczak, M. G. and Russell Iii, J. M. (2018), Understanding the Effects of Polar Mesospheric Clouds on the Environment of the Upper Mesosphere and Lower Thermosphere, *Journal of Geophysical Research: Atmospheres*, *123*(20), 11,705-11,719, https://doi.org/10.1029/2018JD028830.

Smith, A. K. (2012), Global Dynamics of the MLT, *Surveys in Geophysics*, *33*(6), 1177-1230, https://doi.org/10.1007/s10712-012-9196-9.

Sun, M., Lu, J., Li, J., Wei, G., Li, Z., Huang, N. and Zhan, M. (2025), Responses of High-Latitude Mesopause Height and Temperature to Geomagnetic Storms, *Journal of Geophysical Research: Space Physics*, *130*(4), e2024JA033624, https://doi.org/10.1029/2024JA033624.

Tang, C., Liu, D., Wei, H., Wang, Y., Dai, C., Wu, P., Zhu, W. and Rao, R. (2016), The response of the temperature of cold-point mesopause to solar activity based on SABER data set, *Journal of Geophysical Research:Space Physics*, *121*(7), 7245-7255, https://doi.org/10.1002/2016JA022538.

Tapping, K. F. (2013), The 10.7 cm solar radio flux (F10.7), *Space Weather*, *11*(7), 394-406, https://doi.org/10.1002/swe.20064.

Wang, N., Qian, L., Yue, J., Wang, W., Mlynczak, M. G. and Russell Iii, J. M. (2022), Climatology of Mesosphere and Lower Thermosphere Residual Circulations and Mesopause Height Derived From SABER Observations, *Journal of Geophysical Research: Atmospheres*, *127*(4), e2021JD035666, https://doi.org/10.1029/2021JD035666.

Wu, X., Zhu, Y., Smith, A. K., Kaufmann, M., Jiang, G., Liu, S. and Xu, J. (2026), A new data set of nighttime chemical heating rates in the upper mesosphere and lower thermosphere derived from SCIAMACHY OH (9–6) emissions and SABER profiles, *Atmos. Chem. Phys.*, *26*(7), 4669-4683, https://doi.org/10.5194/acp-26-4669-2026.

Xu, J., Smith, A. K., Yuan, W., Liu, H. L., Wu, Q., Mlynczak, M. G. and Russell Iii, J. M. (2007), Global structure and long-term variations of zonal mean temperature observed by TIMED/SABER, *Journal of Geophysical Research: Atmospheres*, *112*(D24), https://doi.org/10.1029/2007JD008546.

Yi, W., Xue, X., Reid, I. M., Murphy, D. J., Hall, C. M., Tsutsumi, M., Ning, B., Li, G., Yang, G., Li, N., Chen, T. and Dou, X. (2021), Climatology of Interhemispheric Mesopause Temperatures Using the High-Latitude and Middle-Latitude Meteor Radars, *Journal of Geophysical Research: Atmospheres*, *126*(6), e2020JD034301, https://doi.org/10.1029/2020JD034301.

Yuan, T., Solomon, S. C., She, C.-Y., Krueger, D. A. and Liu, H.-L. (2019), The Long-Term Trends of Nocturnal Mesopause Temperature and Altitude Revealed by Na Lidar Observations Between 1990 and 2018 at Midlatitude, *Journal of Geophysical Research: Atmospheres*, *124*(12), 5970-5980, https://doi.org/10.1029/2018JD029828.

Zhang, L. and Liu, Z. (2026), A Triple-Structured Mesospheric Climate Pattern Driven by a Double-Celled Meridional Circulation during the Equinox-Solstice Transition Months of November and May, *EGUsphere*, *2026*, 1-32, https://doi.org/10.5194/egusphere-2026-2688.

Zhang, L., Liu, Z. and Tinsley, B. (2025a), Altitude-dependent formation of polar mesospheric clouds: charged nucleation and in situ ice growth on zonal and daily scales, *Atmos. Chem. Phys.*, *25*(19), 12701-12719, https://doi.org/10.5194/acp-25-12701-2025.

Zhang, L., Liu, Z. and Tinsley, B. (2025b), Height-Latitude Patterns of Interannual Climate Variability in the Upper Mesosphere and Lower Thermosphere During Spring and Autumn Months, *Geophysical Research Letters*, *52*(13), e2025GL116281, https://doi.org/10.1029/2025GL116281.

Zhang, L., Liu, Z. and Tinsley, B. (2025c), Interhemispheric Anti-Phase Variability in Mesospheric Climate Driven by Summer Polar Upwelling During Solstice Months, *Atmos. Chem. Phys.*, *25*(20), 13141-13159, https://doi.org/10.5194/acp-25-13141-2025.

Zhang, L., Tinsley, B. and Zhou, L. (2022), Responses of CIPS/AIM noctilucent clouds to the interplanetary magnetic field, *Atmospheric Chemistry and Physics*, *22*(20), 13355-13370, https://doi.org/10.5194/acp-22-13355-2022.

Zhao, X. R., Sheng, Z., Shi, H. Q., Weng, L. B. and Liao, Q. X. (2020), Long-Term Trends and Solar Responses of the Mesopause Temperatures Observed by SABER During the 2002–2019 Period, *Journal of Geophysical Research: Atmospheres*, *125*(11), e2020JD032418, https://doi.org/10.1029/2020JD032418.

Zhou, Q., Friedman, J., Raizada, S., Tepley, C. and Morton, Y. T. (2005), Morphology of nighttime ion, potassium and sodium layers in the meteor zone above Arecibo, *Journal of Atmospheric and Solar-Terrestrial Physics*, *67*(13), 1245-1257, https://doi.org/10.1016/j.jastp.2005.06.013.

Zou, Z., Xue, X., Yi, W., Shen, C., Yang, C., Tang, Y., Chen, T. and Dou, X. (2020), Response of the High-latitude Upper Mesosphere to Energetic Electron Precipitation, *The Astrophysical Journal*, *893*(1), 55, https://doi.org/10.3847/1538-4357/ab7eb0.